Structure-Based Design of a FAAH Variant That Discriminates between the *N*-Acyl Ethanolamine and Taurine Families of Signaling Lipids†

Michele K. McKinney and Benjamin F. Cravatt*

Departments of Cell Biology and Chemistry, The Skaggs Institute for Chemical Biology, The Scripps Research Institute, 10550 North Torrey Pines Road, La Jolla, California 92037

Received April 24, 2006; Revised Manuscript Received June 1, 2006

ABSTRACT: Fatty acid amide hydrolase (FAAH) inactivates a large and diverse class of endogenous signaling lipids termed fatty acid amides. Representative fatty acid amides include the *N*-acyl ethanolamines (NAEs) anandamide, which serves as an endogenous ligand for cannabinoid receptors, and *N*-oleoyl and *N*-palmitoyl ethanolamine, which produce satiety and anti-inflammatory effects, respectively. Global metabolite profiling studies of FAAH (−/−) mice have recently identified a second class of endogenous FAAH substrates: the *N*-acyl taurines (NATs). To determine the metabolic and signaling functions performed by NAEs and NATs in vivo, a FAAH variant that discriminates between these two substrate classes would be of value. Here, we report the structure-guided design of a point mutant in the active site of FAAH that selectively disrupts interactions with NATs. This glycine-to-aspartate (G268D) mutant was found to exhibit wild-type kinetic parameters with NAEs, but more than a 100-fold reduction in activity with NATs attributable to combined effects on K_m and k_{cat} values. These in vitro properties were also observed in living cells, where WT-FAAH and the G268D mutant displayed equivalent hydrolytic activity with NAEs, but the latter enzyme was severely impaired in its ability to catabolize NATs. The G268D FAAH mutant may thus serve as a valuable research tool to illuminate the unique roles played by the NAE and NAT classes of signaling lipids in vivo.

Fatty acid amide hydrolase (FAAH)[1] is a member of the amidase signature (AS) family, a diverse group of metabolic enzymes characterized by a conserved serine- and glycine-rich stretch of approximately 130 amino acids (*1*, *2*). The AS family of hydrolases is found in a wide range of organisms, including archaea (*3*), eubacteria (*1*, *4*−*6*), fungi (*7*), nematodes, plants, insects, birds (*8*), and mammals (*9*, *10*). Unlike most AS enzymes, FAAH is an integral membrane protein (*9*, *10*), which presumably facilitates its role in degrading a large number of amidated lipids in vivo.

The endogenous fatty acid amide substrates hydrolyzed by FAAH fall into multiple structural classes that display distinct biological activities. A principal class of endogenous FAAH substrates is the *N*-acyl ethanolamines (NAEs, Figure 1A), which includes several signaling lipids, such as the endogenous cannabinoid *N*-arachidonoyl ethanolamine or anandamide (C20:4 NAE) (*11*), the satiating factor *N*-oleoyl ethanolamine (C18:1 NAE) (*12*), and the anti-inflammatory substance *N*-palmitoyl ethanolamine (C16:0 NAE) (*13*, *14*).

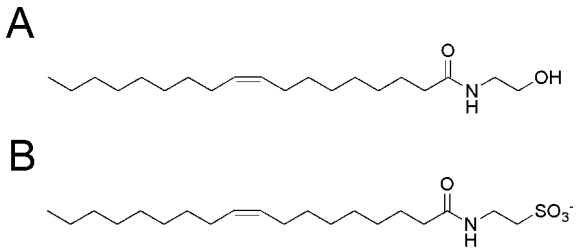

FIGURE 1: Representative FAAH subtrates. (A) *N*-Oleoyl ethanolamine (C18:1 NAE), a representative NAE substrate; (B) *N*-oleoyl taurine (C18:1 NAT), a representative NAT substrate.

FAAH also hydrolyzes fatty acid primary amides, including oleamide, which has been isolated from the cerebrospinal fluid of sleep-deprived cats (*15*) and, upon injection into rats, found to induce physiological sleep (*16*). More recently, global metabolite profiling has been applied to tissues from FAAH(−/−) mice, revealing a third class of substrates, the *N*-acyl taurines (NATs, Figure 1B) (*17*). FAAH regulates complementary sets of NATs in the nervous system and peripheral tissues bearing long chain saturated and polyunsaturated acyl chains, respectively (*17*, *18*). Interestingly, the polyunsaturated NATs controlled by FAAH in the periphery have been found to activate members of the TRP family of cation channels (*18*), suggestive of a signaling function for these lipids.

FAAH(−/−) mice (*19*), as well as FAAH inhibitors (*20*, *21*), have been crucial in establishing a role for this enzyme as a key regulator of fatty acid amide signaling in vivo. FAAH(−/−) mice have highly elevated levels of anandamide

† This work was supported by the National Institutes of Health Grants DA015197 and DA017259 (B.F.C.), the Ruth L. Kirschstein NRSA Predoctoral Fellowship DA019425 (M.K.M.), the Skaggs Institute for Chemical Biology, and the Helen L. Dorris Institute for the Study of Neurological and Psychiatric Disorders of Children and Adolescents.

* To whom correspondence should be addressed. Phone: (858) 784-8633. Fax: (858) 784-8023. E-mail: cravatt@scripps.edu.

[1] Abbreviations: FAAH, fatty acid amide hydrolase; AS, amidase signature; NAE, *N*-acyl ethanolamine; NAT, *N*-acyl taurine; CB1, cannabinoid receptor 1; MAFP, methoxyarachidonyl fluorophosphonate; CA, cytoplasmic access; FP, fluorophosphonate; CAPS, 3-(cyclohexylamino) propanesulfonic acid; SDS−PAGE, sodium dodecyl sulfate−polyacrylamide gel electrophoresis.

10.1021/bi0608010 CCC: $33.50
Published on Web 07/07/2006

and other NAEs in the nervous system that correlate with enhanced brain cannabinoid receptor 1 (CB1) dependent analgesia in these animals (*19*, *22*). FAAH inhibitors also produce CB1-mediated analgesic (*20*, *21*), along with anxiolytic (*20*), effects in rodents. More recently, FAAH(−/−) mice and rodents treated with FAAH inhibitors have been found to display reduced inflammation (*22*−*25*), although, at least in some of these cases, the CB1 receptor does not appear to be involved. These results collectively suggest that the inactivation of FAAH produces two general phenotypes in vivo: those that are CB1-dependent and presumably mediated by anandamide, and those that are CB1-independent and presumably mediated by other fatty acid amides. To elucidate the role that specific classes of FAAH substrates play in regulating the latter set of processes, a strategy to exert independent control over these lipids in vivo would be of great value. With this long-term objective in mind, we describe here the structure-based design and kinetic characterization of a FAAH variant that shows a selective catalytic defect with NAT substrates.

EXPERIMENTAL PROCEDURES

Modeling of FAAH-NAT Complexes. C20:4 NAT was modeled into the FAAH active site using the existing X-ray crystal structure (PDB: 1MT5) of the enzyme in covalent complex with a methoxyarachidonyl fluorophosphonate inhibitor (MAFP) (*26*). The acyl chain of the NAT substrate and alkyl chain of the MAFP inhibitor, both C20:4, were overlayed, and the carbonyl carbon of C20:4 NAT was modeled in place of the MAFP phosphate. The taurine group of the substrate was modeled using Python Molecular Viewer (*27*) and placed to minimize steric clashes with the FAAH active site.

Expression and Purification of Wild-Type (WT) and Mutant FAAH Enzymes. For in vitro kinetic studies, rat FAAH proteins were recombinantly expressed in *Escherichia coli* strain BL21(DE3) as *N*-terminal His_6-tag fusion proteins and purified by sequential metal affinity, heparin agarose, and gel filtration chromatography, as described previously (*28*). All point mutants were generated using the QuikChange procedure (Stratagene) and were verified by sequencing the entire coding region. FAAH proteins contained an *N*-terminal truncation of amino acid residues 1−29, which constitute a predicted transmembrane domain. This deletion has been shown to have no effect on catalytic activity or membrane binding, but enhances expression and purification (*28*). For clarity, numbered residues refer to the full-length FAAH protein. Enzyme concentrations were calculated assuming an absorbance at 280 nm of 0.8 AU for a 1 mg/mL solution of FAAH (*28*). Purified protein was stored at −80 °C in 10% glycerol until used for in vitro assays.

Synthesis of FAAH Substrates. NAEs were synthesized by a reaction of their respective acid chlorides with ethanolamine as described previously (*9*). NATs were synthesized by a reaction of their respective acid chlorides with taurine in TEA and dioxane as described previously (*17*).

Circular Dichroism Spectrometry. Protein samples at 0.5 mg/mL (7.75 μM) in 10 mM Tris, pH 8.0, 100 mM NaCl, and 0.015% lauryldimethylamine oxide were measured by far-UV circular dichroism at 25 °C in a 0.1 cm cell on an Aviv stopped-flow CD spectrometer.

Table 1: Rates of Labeling by FP-Rhodamine

	$k_{obs}/[I]$ ($M^{-1}\,s^{-1}$)
FAAH	$(2.8 \pm 0.1) \times 10^5$
G268D	$(3.0 \pm 0.2) \times 10^5$

Fluorophosphonate Labeling. Rates of fluorophosphonate inhibitor labeling were measured as previously described (*29*). Briefly, labeling reactions of 10 nM enzyme and 0.1 μM fluorophosphonate-tetramethyl rhodamine [FP-rhodamine (*30*)] were allowed to proceed at 25 °C for 5, 10, and 20 min using the reaction buffer above at pH 7.0 and quenched with 1 vol of 2× SDS loading buffer. Control samples of WT-FAAH were labeled to completion and used as a reference for 100% reactivity. Quenched reactions were subsequently analyzed by SDS−PAGE with 0.15 pmol protein/gel lane. The extent of FP-labeling was visualized in-gel using a Hitachi FMBio IIe flatbed laser-induced fluorescence scanner and quantified by measuring the integrated fluorescence band intensities (*29*). Values for FP-labeling are reported as the second-order rate constant $k_{obs}/[I]$, where [I] is the concentration of FP-rhodamine. For each mutant enzyme, similar $k_{obs}/[I]$ values were obtained at 5 and 10 min time points, and these values were averaged from triplicate trials to provide the values reported in Table 1.

LC−MS Analysis. LC−MS analysis (*18*) was performed using an Agilent 1100 LC/MSD SL instrument. A Gemini (Phenomenex) C18 reverse-phase column (5 μm, 4.6 × 100 mm) was used together with a precolumn (C18, 3.5 μm, 2 × 20 mm). Mobile phase A consisted of 95/5 water/methanol, and mobile phase B was made up of 60/35/5 2-propanol/methanol/water. Both A and B were supplemented with 0.1% ammonium hydroxide as solvent modifiers. The gradient started at 40% B and then linearly increased to 100% B over 10 min. MS analysis was performed with an electrospray source ionization (ESI) interface. The capillary voltage was set to 3.0 kV and the fragmentor voltage to 100 V. The drying gas temperature was 350 °C, the drying gas flow was 10 L/min, and the nebulizer pressure was 35 psi.

In Vitro WT- and G268D-FAAH Catalytic Activity Assays. For C18:1 NAE and NAT, FAAH activity assays were performed by following the conversion of [^{14}C]-substrates to oleic acid using a thin-layer chromatography (TLC) assay as described previously (*28*). Reactions were conducted in a buffer of 50 mM Bis-Tris propane, 50 mM CAPS, 50 mM citrate, 150 mM NaCl, and 0.05% Triton X-100. The pH of the buffer was adjusted using HCl or NaOH. Reactions were quenched with 0.5 N HCl at four time points. Oleic acid was separated from C18:1 NAE and NAT by TLC in 70% ethyl acetate/30% hexanes. The radioactive compounds were quantified using a Cyclone PhosphorImager (Perkin-Elmer Life Sciences).

FAAH assays with C20:4 NAE and NAT were performed with unlabeled substrates in the aforementioned buffer and quenched similarly. Arachidonic acid production was measured by LC−MS (analysis conditions described above) using the peak area under the extracted ion chromatogram and quantified by comparison to a standard product curve (0−250 pmol C20:4 fatty acid) as described (*17*, *18*).

For all substrate reactions, time courses were chosen such that product formation did not exceed 20%. Over this time

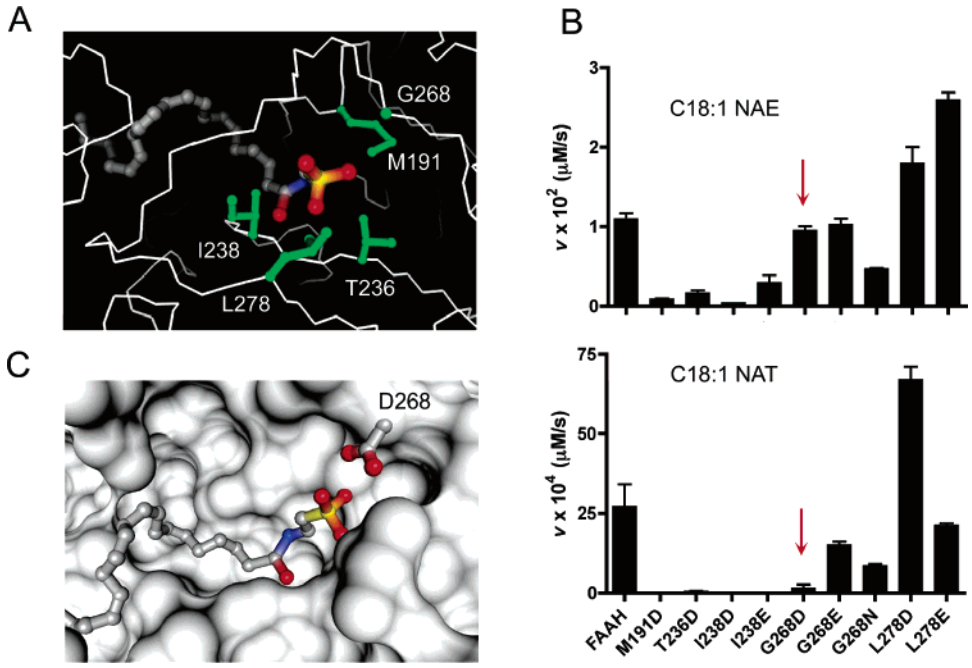

FIGURE 2: Characterization of FAAH variants with aspartate or glutamate mutations in the CA channel. (A) Residues near the taurine headgroup of a modeled complex of C20:4 NAT and FAAH that targeted for mutagenesis to glutamate or aspartate. (B) Hydrolytic activities of FAAH mutants measured with C18:1 NAE and NAT substrates. (C) Model of C20:4 NAT in the G268D-FAAH active site. The C20:4 NAT substrate and G268D mutation were modeled into the FAAH active site by modifying the existing crystal structure of a FAAH−MAFP complex (*26*) [PDB: 1MT5, rendered using Python Molecular Viewer (*27*)].

range, FAAH enzymes showed linear reaction kinetics. Apparent K_m and k_{cat} values were calculated from either Lineweaver−Burk or Michaelis−Menten plots of four substrate concentrations run in triplicate. Because saturating conditions with the C20:4 NAT substrate could not be attained with the G268D-FAAH variant, the apparent second-order rate constant, k_{cat}/K_m, was determined from reaction rate (v) versus substrate concentration [S] plots. This calculation assumes that substrate concentration is much lower than K_m, which appeared to be the case for G268D-FAAH as the enzyme displayed constant v/[S] values for C20:4 NAT over the entire tested range of substrate concentrations (25−200 μM).

In Situ Analysis of WT- and G268D-FAAH Activity. Studies in living COS-7 cells utilized full-length rat FAAH proteins expressed by transient transfection as described previously (*9*). COS-7 cells were transfected at approximately 75% confluency using Fugene6 (Roche), and in situ FAAH activities were assayed on the second day following transfection. [^{13}C]-18:1 NAE and NAT were added to 5 mL of complete medium (DMEM with L-glutamine, sodium pyruvate, and 10% fetal bovine serum) for a final concentration of 10 μM substrate. The resulting solution was added to 10 cm dishes of transfected COS-7 cells transfected with either WT- or G268D-FAAH cDNAs in the pcDNA3.1 vector (Invitrogen). Mock-transfected cells (transfected with empty pcDNA3.1 vector) were used as a control to estimate background FAAH activity. Following a 10 min incubation at 37 °C, the medium was removed, and cells were washed with 2 × 5 mL of complete medium and harvested by scraping. Cell suspensions were extracted with chloroform/methanol (2:1), and the organic layers were removed and dried under a nitrogen stream. Dried organic extracts were resuspended in 200 μL methanol and analyzed by LC−MS using single ion monitoring to measure the amount of ^{13}C-oleic acid product formed. Results were quantified by measuring the peak area of the extracted ion chromatogram against a standard curve of oleic acid.

RESULTS

Characterization of Cytoplasmic Access (CA) Tunnel Mutants of FAAH. We hypothesized that the development of FAAH mutants showing reduced activity with NATs might be accomplished by mutating neutral residues in the proposed cytoplasmic access (CA) tunnel of the enzyme to negatively charged residues (aspartic and glutamic acid). This tunnel was chosen for focused mutagenesis because it has been proposed to function as a route for release of the hydrophilic amine leaving groups of amidated substrates (*26*). By introducing negatively charged residues into the CA tunnel, we hoped to selectively impair the binding and hydrolysis of NATs due to charge−charge repulsion with the taurine sulfonate group.

Modeling the binding of NATs in the FAAH active site, where the cleaved amide group was positioned to interact with the S241 nucleophile, highlighted several residues with predicted proximity to the NAT sulfate: M191, T236, I238, G268, and L278 (Figure 2A). Each of these residues was mutated to either aspartate or glutamate, and the resulting FAAH mutants were recombinantly expressed in *E. coli* as His_6-tagged fusion proteins and purified as described previously (*28*). With the exceptions of M191E and T236E, all of the designed FAAH mutants expressed to sufficiently high levels to permit kinetic analysis. The purified FAAH mutants were screened for activity using substrate hydrolysis assays (10 nM FAAH protein, 100 μM C18:1 NAE or NAT substrate). Most of these mutants displayed either no defects in catalysis with NAE or NAT substrates or reductions in

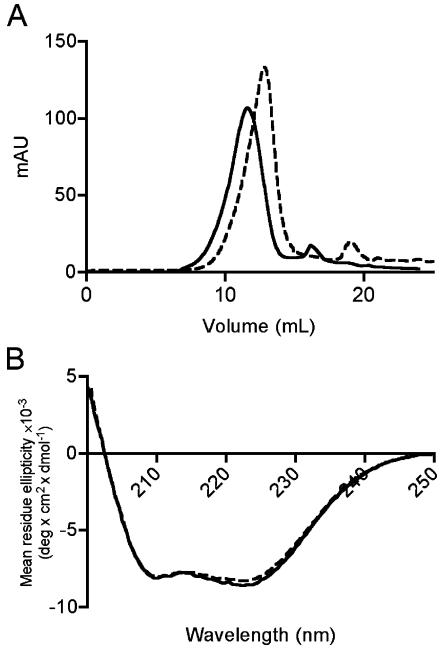

FIGURE 3: WT- and G268D-FAAH exhibit similar biophysical properties. (A) Gel filtration elution profile of WT-FAAH (solid line) and G268D-FAAH (dashed line). (B) Far-UV circular dichroism of WT-FAAH (solid line) and G268D-FAAH (dashed line).

hydrolysis with both substrates compared to WT-FAAH (Figure 2B). However, one mutant, the G268D-FAAH enzyme, displayed a marked decrease in hydrolysis with C18:1 NAT (>10-fold), while maintaining wild-type activity with C18:1 NAE (Figure 2B, red arrow). Another mutation, L278E, also resulted in a modest decrease (~1.7-fold) in NAT hydrolysis. A FAAH variant containing the double mutation G268D/L278E was generated, but further kinetic analyses were not performed due to the very poor expression levels of this protein (data not shown).

Biochemical Characterization of the G268D-FAAH Mutant. Modeling studies indicated that the aspartate residue introduced in G268D-FAAH could reside within 3 Å of the sulfonate group of NATs (Figure 2C), which would make it well-positioned to selectively disrupt the productive binding of these negatively charged substrates. Consistent with this model of charge−charge repulsion, a G268N-FAAH mutant was found to exhibit equivalent relative, albeit slightly reduced, overall activity with both NAE and NAT substrates compared to WT-FAAH (Figure 2B).

Table 4: Ratios of k_{cat}/K_m FAAH: k_{cat}/K_m G268D for NAEs and NATs

k_{cat}/K_m	C18:1 NAE	C18:1 NAT	C20:4 NAE	C20:4 NAT
FAAH: G268D	0.23 ± 0.07	133 ± 5	1.3 ± 0.5	$(1.5 \pm 0.5) \times 10^3$

G268D-FAAH was found to express at similar levels to WT-FAAH, with both enzymes yielding 0.5−1.0 mg of purified enzyme per liter of *E. coli* culture volume. WT- and G268D-FAAH also displayed equivalent gel filtration elution and far-UV circular dichroism profiles (Figure 3), as well as similar rates of reactivity with a rhodamine-tagged FP (FP-rhodamine) probe (Table 1). These data indicate that G268D-FAAH is a well-folded enzyme that possesses a fully functional S241 nucleophile. We therefore proceeded with a more detailed kinetic characterization of this FAAH variant.

Comparative Characterization of the Catalytic Properties of WT- and G268D-FAAH. Kinetic parameters for WT- and G268D-FAAH were compared using purified, recombinant enzymes and representative monounsaturated (C18:1) and polyunsaturated (C20:4) members of the NAE and NAT classes of endogenous substrates. Assays were conducted in the presence of detergent (0.05% Triton X-100) and organic cosolvent (5% DMSO) to maintain enzymes and substrates in solution. As is summarized in Tables 2 and 3, WT-FAAH displayed moderately higher (4−7-fold) specificity constants (k_{cat}/K_m) for C18:1 and C20:4 NAEs compared to the corresponding NATs, which was mostly due to differences in k_{cat}. In contrast, the G268D mutant, which showed near wild-type kinetic parameters with NAE substrates, exhibited more than a 100-fold reduction in k_{cat}/K_m values for both the C18:1 and C20:4 NATs (Tables 2−4). These impairments in catalytic activity for the G268D mutant were reflected in both k_{cat} and K_m values for C18:1 NAT (Table 2). In the case of C20:4 NAT, saturation kinetics with the G268D mutant were not observed up to 200 μM substrate, setting a lower limit on K_m that was at least 20-fold higher than the wild-type value (8 μM) (Table 3). Finally, the G268D-FAAH variant showed wild-type rates of hydrolysis with oleamide (0.027 ± 0.005 μM/s compared to 0.032 ± 0.006 μM/s for WT-FAAH; 100 μM substrate), indicating that the G268D

Table 2: Catalytic Properties of G268D FAAH with C18:1 NAE and C18:1 NAT[a]

	C18:1 NAE			C18:1 NAT			NAE:NAT
	K_m (μM)	k_{cat} (s^{-1})	k_{cat}/K_m ($M^{-1}\,s^{-1}$)	K_m (μM)	k_{cat} (s^{-1})	k_{cat}/K_m ($M^{-1}\,s^{-1}$)	k_{cat}/K_m ratio
FAAH	12 ± 4	0.85 ± 0.07	$(7 \pm 2) \times 10^4$	17 ± 3	0.29 ± 0.04	$(1.67 \pm 0.05) \times 10^4$	4
G268D	3.2 ± 0.4	0.95 ± 0.03	$(3.0 \pm 0.4) \times 10^5$	131 ± 6	0.016 ± 0.001	126 ± 3	2400

[a] In vitro assays were conducted in the presence of detergent, and the reported kinetic parameters are therefore apparent values.

Table 3: Catalytic Properties of G268D FAAH with C20:4 NAE and C20:4 NAT[a]

	C20:4 NAE			C20:4 NAT			NAE:NAT
	K_m (μM)	k_{cat} (s^{-1})	k_{cat}/K_m ($M^{-1}\,s^{-1}$)	K_m (μM)	k_{cat} (s^{-1})	k_{cat}/K_m ($M^{-1}\,s^{-1}$)	k_{cat}/K_m ratio
FAAH	17 ± 3	4.8 ± 0.3	$(2.8 \pm 0.5) \times 10^5$	8 ± 3	0.30 ± 0.01	$(4 \pm 1) \times 10^4$	7
G268D	6 ± 2	1.30 ± 0.08	$(2.2 \pm 0.8) \times 10^5$	>200		27 ± 5	8000

[a] In vitro assays were conducted in the presence of detergent, and the reported kinetic parameters are therefore apparent values.

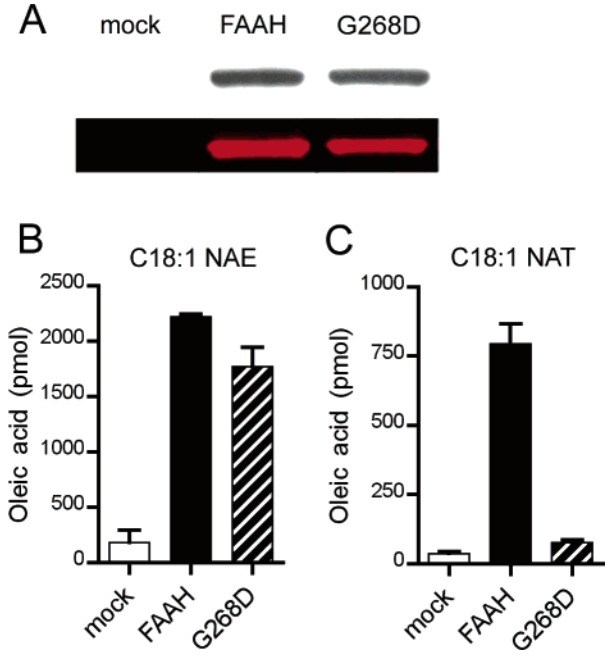

FIGURE 4: Comparison of the in situ hydrolytic activities of WT- and G268D-FAAH. (A) WT- and G268D-FAAH transfected COS-7 cells possess similar levels of FAAH protein, as judged by Western blotting (upper panel) and FP-rhodamine labeling (lower panel). (B) WT- and G268D-FAAH transfected cells show similar hydrolytic activities with C18:1 NAE, which are both much greater than the activity observed in mock-transfected cells. (C) WT-FAAH transfected cells show much greater hydrolysis activity with C18:1 NAT compared to either G268D-FAAH or mock-transfected cells.

mutation did not adversely affect interactions with substrates of the primary fatty acid amide class.

Overall, the selective catalytic defects displayed by the G268D mutant resulted in a more than 2000-fold reduction in relative k_{cat}/K_m values for NATs compared to NAEs (Tables 2 and 3). We next asked whether these alterations in substrate selectivity of G268D-FAAH observed in vitro would be maintained in living systems.

Comparative Characterization of the Hydrolytic Activities of WT- and G268D-FAAH in Living Cells. The in vitro analysis of the catalytic properties of WT- and G268D-FAAH was conducted under conditions that are quite different from those found in living cells, where FAAH and, presumably, its substrates are integrated into membranes. A more physiologically relevant assay was therefore sought to characterize the substrate selectivities of WT- and G268D-FAAH. The in situ activities of WT- and G268D-FAAH were compared in transiently transfected COS-7 cells by monitoring the conversion of C18:1 NAE and NAT to oleic acid. WT- and G268D-FAAH transfected cells possessed similar levels of FAAH protein as judged by Western blotting and FP-rhodamine reactivity (Figure 4A). Initial time-course studies with 10 μM C18:1 NAE indicated that the rate of production of oleic acid by WT-FAAH transfected cells was linear up to 15 min of incubation. Therefore, hydrolytic activities were compared following a 10 min incubation with substrates. WT- and G268D-FAAH transfected cells showed nearly equivalent levels of hydrolysis of C18:1 NAE that were much higher than mock-transfected cells (Figure 4B). In contrast, WT-FAAH transfected cells exhibited much greater hydrolytic activity with C18:1 NAT compared to G268D-FAAH transfected cells, which hydrolyzed C18:1 NAT at a level comparable to that of mock-transfected cells (Figure 4C). These studies indicate that the altered substrate selectivity of the G268D-FAAH mutant is preserved in living cells.

DISCUSSION

The recent discovery of a novel class of natural FAAH substrates, the *N*-acyl taurines (NATs), has broadened our perspective on the catabolic roles that this enzyme plays in vivo (*17*, *18*). The further characterization of NATs as candidate endogenous ligands for the calcium channels TRPV1 and TRPV4 suggests that disruption of FAAH function in vivo could produce effects that extend beyond those mediated by the endocannabinoid anandamide and other NAEs (*18*). Consistent with this notion, FAAH(−/−) mice show certain phenotypes (e.g., anti-inflammation) that are not blocked by cannabinoid receptor antagonists (*24*). Elucidation of the molecular basis for phenotypes that accompany FAAH inactivation would benefit from advanced model systems in which the levels of distinct sets of FAAH substrates could be independently controlled in vivo. Here, we have described progress toward this goal in the form of an active site mutant of FAAH that shows selective impairment in catalytic activity with NATs.

Mutagenesis in the proposed CA tunnel of FAAH was performed to investigate (1) whether this region was involved in binding the amine leaving groups of FAAH substrates, and if so, (2) whether the introduction of negatively charged residues into the CA tunnel would selectively impair productive interactions with NAT substrates. Protein engineering based on electrostatic interactions between charged substrates and neighboring amino acids in enzyme active sites has been previously demonstrated. For example, Wells and colleagues showed that the specificity constant (k_{cat}/K_m) of the protease subtilisin BPN′ could be substantially increased or decreased by introducing complementary or similarly charged substitutions in substrate/enzyme pairs, respectively (*31*). The mutagenesis of amino acids surrounding a lipid headgroup to confer changes in substrate specificity also bears some precedent. Phosphatidylcholine-preferring phospholipase C from *Bacillus cereus* has three key amino acids that form the choline binding pocket, and alterations of these amino acids yield enzyme variants that are either phosphatidylethanolamine- or phosphatidylserine-preferring (*32*, *33*). On the basis of these precedents, a series of FAAH mutants bearing additional glutamate or aspartate residues in the CA tunnel was generated with the aim of selectively decreasing activity with NATs due to repulsive interactions with the negatively charged taurine headgroup of these substrates. A G268D-FAAH mutant emerged from this analysis as an enzyme that could discriminate between NAE and NAT substrates.

G268D-FAAH exhibited severe catalytic defects with NAT substrates that were due to a combination of effects on K_m and k_{cat} values. Similar results were obtained with NATs bearing different acyl chains (C18:1 and C20:4), supporting the concept that perturbed interactions with the taurine leaving group were predominantly responsible for the observed reductions in catalysis. In contrast, kinetic parameters with NAE substrates were largely unaffected by the G268D mutation. Thus, FAAH's hydrolytic efficiency for NAE and NAT substrates was successfully uncoupled by a single active site mutation.

The ultimate goal of disassociating FAAH's capacity to hydrolyze NAEs and NATs is to provide model systems to separately study the function of these two classes of bioactive lipids in vivo. Toward this end, a comparison of WT- and G268D-FAAH in transfected COS-7 cells revealed similar in situ hydrolytic activities with NAEs, but a profound defect in NAT hydrolysis for the latter enzyme. If these metabolic phenotypes are preserved in living animals, then a "knock-in" mouse that expresses G268D-FAAH may be expected to possess wild-type levels of NAEs, but constitutively elevated concentrations of NATs. Efforts toward the generation of this animal model and an assessment of its metabolic and physiological phenotypes are underway.

ACKNOWLEDGMENT

We thank A. Saghatelian for providing NAT substrates and for helpful discussion, M. Bracey for assistance with FAAH figures, and J. Kelly and J. Suk for use of the CD spectrophotometer.

REFERENCES

1. Mayaux, J. F., Cerebelaud, E., Soubrier, F., Faucher, D., and Petre, D. (1990) Purification, cloning, and primary structure of an enantiomer-selective amidase from *Brevibacterium* sp. strain R312: structural evidence for genetic coupling with nitrile hydratase, *J. Bacteriol. 172*, 6764−6773.
2. Chebrou, H., Bigey, F., Arnaud, A., and Galzy, P. (1996) Study of the amidase signature group, *Biochim. Biophys. Acta 1298*, 285−293.
3. Sako, Y., Nomura, N., Uchida, A., Ishida, Y., Morii, H., Koga, Y., Hoaki, T., and Maruyama, T. (1996) *Aeropyrum pernix* gen. nov., sp. nov., a novel aerobic hyperthermophilic archaeon growing at temperatures up to 100 degrees C, *Int. J. Syst. Bacteriol. 46*, 1070−1077.
4. Kobayashi, M., Komeda, H., Nagasawa, T., Nishiyama, M., Horinouchi, S., Beppu, T., Yamada, H., and Shimizu, S. (1993) Amidase coupled with low-molecular-mass nitrile hydratase from *Rhodococcus rhodochrous* J1. Sequencing and expression of the gene and purification and characterization of the gene product, *Eur. J. Biochem. 217*, 327−336.
5. Boshoff, H. I., and Mizrahi, V. (1998) Purification, gene cloning, targeted knockout, overexpression, and biochemical characterization of the major pyrazinamidase from *Mycobacterium smegmatis*, *J. Bacteriol. 180*, 5809−5814.
6. Hashimoto, Y., Nishiyama, M., Ikehata, O., Horinouchi, S., and Beppu, T. (1991) Cloning and characterization of an amidase gene from *Rhodococcus* species N-774 and its expression in *Escherichia coli*, *Biochim. Biophys. Acta 1088*, 225−233.
7. Gomi, K., Kitamoto, K., and Kumagai, C. (1991) Cloning and molecular characterization of the acetamidase-encoding gene (amdS) from *Aspergillus oryzae*, *Gene 108*, 91−98.
8. Ettinger, R. A., and DeLuca, H. F. (1995) The vitamin D3 hydroxylase-associated protein is a propionamide-metabolizing amidase enzyme, *Arch. Biochem. Biophys. 316*, 14−19.
9. Cravatt, B. F., Giang, D. K., Mayfield, S. P., Boger, D. L., Lerner, R. A., and Gilula, N. B. (1996) Molecular characterization of an enzyme that degrades neuromodulatory fatty-acid amides, *Nature 384*, 83−87.
10. Giang, D. K., and Cravatt, B. F. (1997) Molecular characterization of human and mouse fatty acid amide hydrolases, *Proc. Natl. Acad. Sci. U.S.A. 94*, 2238−2242.
11. Devane, W. A., Hanus, L., Breuer, A., Pertwee, R. G., Stevenson, L. A., Griffin, G., Gibson, D., Mandelbaum, A., Etinger, A., and Mechoulam, R. (1992) Isolation and structure of a brain constituent that binds to the cannabinoid receptor, *Science 258*, 1946−1949.
12. Fu, J., Gaetani, S., Oveisi, F., Lo Verme, J., Serrano, A., Rodriguez De Fonseca, F., Rosengarth, A., Luecke, H., Di Giacomo, B., Tarzia, G., and Piomelli, D. (2003) Oleylethanolamide regulates feeding and body weight through activation of the nuclear receptor PPAR-alpha, *Nature 425*, 90−93.
13. Calignano, A., La Rana, G., Giuffrida, A., and Piomelli, D. (1998) Control of pain initiation by endogenous cannabinoids, *Nature 394*, 277−281.
14. Jaggar, S. I., Hasnie, F. S., Sellaturay, S., and Rice, A. S. (1998) The anti-hyperalgesic actions of the cannabinoid anandamide and the putative CB2 receptor agonist palmitoylethanolamide in visceral and somatic inflammatory pain, *Pain 76*, 189−199.
15. Lerner, R. A., Siuzdak, G., Prospero-Garcia, O., Henriksen, S. J., Boger, D. L., and Cravatt, B. F. (1994) Cerebrodiene: a brain lipid isolated from sleep-deprived cats, *Proc. Natl. Acad. Sci. U.S.A. 91*, 9505−9508.
16. Cravatt, B. F., Prospero-Garcia, O., Siuzdak, G., Gilula, N. B., Henriksen, S. J., Boger, D. L., and Lerner, R. A. (1995) Chemical characterization of a family of brain lipids that induce sleep, *Science 268*, 1506−1509.
17. Saghatelian, A., Trauger, S. A., Want, E. J., Hawkins, E. G., Siuzdak, G., and Cravatt, B. F. (2004) Assignment of endogenous substrates to enzymes by global metabolite profiling, *Biochemistry 43*, 14332−14339.
18. Saghatelian, A., McKinney, M. K., Bandell, M., Patapoutian, A., and Cravatt, B. F. (2006) A FAAH-regulated class of *N*-acyl taurines that activates TRP ion channels, *Biochemistry*, *45*, 9007−9015.
19. (a) Cravatt, B. F., Demarest, K., Patricelli, M. P., Bracey, M. H., Giang, D. K., Martin, B. R., and Lichtman, A. H. (2001) Supersensitivity to anandamide and enhanced endogenous cannabinoid signaling in mice lacking fatty acid amide hydrolase, *Proc. Natl. Acad. Sci. U.S.A. 98*, 9371−9376.
20. Kathuria, S., Gaetani, S., Fegley, D., Valino, F., Duranti, A., Tontini, A., Mor, M., Tarzia, G., La Rana, G., Calignano, A., Giustino, A., Tattoli, M., Palmery, M., Cuomo, V., and Piomelli, D. (2003) Modulation of anxiety through blockade of anandamide hydrolysis, *Nat. Med. 9*, 76−81.
21. Lichtman, A. H., Leung, D., Shelton, C., Saghatelian, A., Hardouin, C., Boger, D., and Cravatt, B. F. (2004) Reversible inhibitors of fatty acid amide hydrolase that promote analgesia: evidence for an unprecedented combination of potency and selectivity, *J. Pharmacol. Exp. Ther. 311*, 441−448.
22. Lichtman, A. H., Shelton, C. C., Advani, T., and Cravatt, B. F. (2004) Mice lacking fatty acid amide hydrolase exhibit a cannabinoid receptor-mediated phenotypic hypoalgesia, *Pain 109*, 319−327.
23. Cravatt, B. F., Saghatelian, A., Hawkins, E. G., Clement, A. B., Bracey, M. H., and Lichtman, A. H. (2004) Functional disassociation of the central and peripheral fatty acid amide signaling systems, *Proc. Natl. Acad. Sci. U.S.A. 101*, 10821−10826.
24. Massa, F., Marsicano, G., Hermann, H., Cannich, A., Monory, K., Cravatt, B. F., Ferri, G. L., Sibaev, A., Storr, M., and Lutz, B. (2004) The endogenous cannabinoid system protects against colonic inflammation, *J. Clin. Invest. 113*, 1202−1209.
25. Holt, S., Comelli, F., Costa, B., and Fowler, C. J. (2005) Inhibitors of fatty acid amide hydrolase reduce carrageenan-induced hind paw inflammation in pentobarbital-treated mice: comparison with indomethacin and possible involvement of cannabinoid receptors, *Br. J. Pharmacol. 146*, 467−476.
26. Bracey, M. H., Hanson, M. A., Masuda, K. R., Stevens, R. C., and Cravatt, B. F. (2002) Structural adaptations in a membrane enzyme that terminates endocannabinoid signaling, *Science 298*, 1793−1796.
27. Sanner, M. F. (1999) Python: a programming language for software integration and development, *J. Mol. Graphics Modell. 17*, 57−61.
28. Patricelli, M. P., Lashuel, H. A., Giang, D. K., Kelly, J. W., and Cravatt, B. F. (1998) Comparative characterization of a wild type and transmembrane domain-deleted fatty acid amide hydrolase: identification of the transmembrane domain as a site for oligomerization, *Biochemistry 37*, 15177−15187.
29. McKinney, M. K., and Cravatt, B. F. (2003) Evidence for distinct roles in catalysis for residues of the serine-serine-lysine catalytic triad of fatty acid amide hydrolase, *J. Biol. Chem. 278*, 37393−37399.
30. Patricelli, M. P., Giang, D. K., Stamp, L. M., and Burbaum, J. J. (2001) Direct visualization of serine hydrolase activities in complex proteomes using fluorescent active site-directed probes, *Proteomics 1*, 1067−1071.

31. Wells, J. A., Powers, D. B., Bott, R. R., Graycar, T. P., and Estell, D. A. (1987) Designing substrate specificity by protein engineering of electrostatic interactions, *Proc. Natl. Acad. Sci. U.S.A. 84*, 1219−1223.
32. Martin, S. F., Follows, B. C., Hergenrother, P. J., and Trotter, B. K. (2000) The choline binding site of phospholipase C (*Bacillus cereus*): insights into substrate specificity, *Biochemistry 39*, 3410−3415.
33. Antikainen, N. M., Hergenrother, P. J., Harris, M. M., Corbett, W., and Martin, S. F. (2003) Altering substrate specificity of phosphatidylcholine-preferring phospholipase C of *Bacillus cereus* by random mutagenesis of the headgroup binding site, *Biochemistry 42*, 1603−1610.

BI0608010